J Biomol NMR (2016) 65:121–126
DOI 10.1007/s10858-016-0044-y

COMMUNICATION

High resolution observed in 800 MHz DNP spectra of extremely rigid type III secretion needles

Pascal Fricke[1] · Deni Mance[2] · Veniamin Chevelkov[1] · Karin Giller[3] · Stefan Becker[3] · Marc Baldus[2] · Adam Lange[1,4]

Received: 29 April 2016 / Accepted: 22 June 2016 / Published online: 28 June 2016

Abstract The cryogenic temperatures at which dynamic nuclear polarization (DNP) solid-state NMR experiments need to be carried out cause line-broadening, an effect that is especially detrimental for crowded protein spectra. By increasing the magnetic field strength from 600 to 800 MHz, the resolution of DNP spectra of type III secretion needles (T3SS) could be improved by 22 %, indicating that inhomogeneous broadening is not the dominant effect that limits the resolution of T3SS needles under DNP conditions. The outstanding spectral resolution of this system under DNP conditions can be attributed to its low overall flexibility.

Keywords Proteins · Type III Secretion System · Solid-State NMR · DNP · Dynamics · PRE

Electronic supplementary material The online version of this article (doi:10.1007/s10858-016-0044-y) contains supplementary material, which is available to authorized users.

✉ Adam Lange
alange@fmp-berlin.de

[1] Department of Molecular Biophysics, Leibniz-Institut für Molekulare Pharmakologie, 13125 Berlin, Germany

[2] NMR Research Group, Bijvoet Center for Biomolecular Research, Utrecht University, 3584 CH Utrecht, The Netherlands

[3] Department of NMR-Based Structural Biology, Max Planck Institute for Biophysical Chemistry, 37077 Göttingen, Germany

[4] Institut für Biologie, Humboldt-Universität zu Berlin, 10115 Berlin, Germany

Content

To overcome the inherent insensitivity of NMR in the solid state by hyperpolarization, dynamic nuclear polarization (DNP) has become the most promising approach to date (Barnes et al. 2008; Lee et al. 2015). It has been shown that DNP can drastically increase the sensitivity in solid-state NMR (ssNMR) experiments (Ni et al. 2013; Sauvee et al. 2013; Song et al. 2006) and it has been successfully applied to several biological systems (Becker-Baldus et al. 2015; Debelouchina et al. 2013; Fricke et al. 2015; Gupta et al. 2016; Kaplan et al. 2015; Koers et al. 2014; Potapov et al. 2015). Unfortunately, those experiments need to be carried out at cryogenic temperatures as the enhancement factor decreases with increasing temperature (Rosay et al. 2010; Sauvee et al. 2013; Zagdoun et al. 2013). At ambient temperatures, at which standard protein ssNMR experiments are conducted, the enhancement is negligible.

At usual DNP temperatures (~100 K) different conformations of the protein are frozen out. This aspect can result in severe line-broadening due to the overlapping peaks of the individual conformers which exhibit different chemical shifts (inhomogeneous line-broadening) (Linden et al. 2011; Siemer et al. 2012). Indeed, previous work has found a remarkable correlation between experimentally observed ^{13}Ca line-width and protein backbone fluctuations as predicted from molecular dynamics (MD) simulations (Koers et al. 2014). Additionally, there is homogeneous line-broadening, which, for example, is caused by the proximity of the biradicals (Koers et al. 2014; van der Cruijsen et al. 2015). In the crowded NMR spectra of proteins (Shi et al. 2015), these effects are highly undesired and make the analysis of such spectra extremely difficult. Furthermore, broad lines lead to a loss of sensitivity, as the signal intensity at a given peak volume reduces with the

line-width and thus the sensitivity advantage provided by DNP is lowered (Takahashi et al. 2012). This effect becomes more severe when recording higher-dimensional spectra, where the line-broadening "penalty" has to be paid for each dimension.

Improving the resolution is therefore a principal goal to fully exploit the advantages of the increased sensitivity conveyed by DNP. This can be achieved by searching for different sample preparation protocols rather than using the established glycerol matrix (Liao et al. 2016; Takahashi et al. 2013) and by searching for biradicals that allow reasonable enhancement factors at higher temperatures (Lelli et al. 2015; Perras et al. 2016).

Another option is to increase the magnetic field strength (Koers et al. 2014). A higher magnetic field would in principle not be expected to considerably reduce the line-width in case it is dominated by inhomogeneous broadening. For example, such a situation would occur in the presence of overlapping conformer peaks as they are distributed in terms of their chemical shift, which is directly proportional to the external magnetic field. Only the homogeneously broadened part scales with Hz and thus results in improved resolution at higher fields.

In samples where structural heterogeneity is not the limiting factor, it has been shown (Lopez del Amo et al. 2013) that the resolution at cryogenic temperatures improves considerably when increasing the external magnetic field strength. Here, we observed a considerable improvement in resolution when comparing two DNP ^{13}C-^{13}C proton-driven spin diffusion (PDSD) 2D NMR spectra of the same protein acquired at magnetic fields of 600 and 800 MHz (Fig. 1). The ^{13}C-^{13}C correlation via supercycled POST-C5 (SPC-5) (Hohwy et al. 1999) is shown in Fig. S1 (supplementary material).

The studied sample consists of T3SS needles formed by the supramolecular assembly of the 83-amino acid protein MxiH (Demers et al. 2014, 2013). The preparation is described and illustrated (Fig. S2) in the supplementary material.

In a previous study conducted at 600 MHz (Fricke et al. 2014), this system exhibited one of the best resolutions ever achieved for a protein sample under DNP conditions (Can et al. 2015; Su et al. 2015). Increasing the field strength to 800 MHz and using the biradical AMUPol (Sauvee et al. 2013), the observed line-widths at half height are about 22 % smaller, improving the overall resolution of the spectrum sizably. In the previous study based on the biradical TOTAPOL (Song et al. 2006), an enhancement of 23 was observed at 600 MHz. In the new study using AMUPol at 800 MHz, we obtained an enhancement factor of 21 (Fig. S3 in the supplementary material).

The fact that this protein assembly shows such well-resolved DNP spectra is most likely caused by the overall stiffness of the needle structure and the resulting reduced dynamics: A structurally nearly identical and homologous (>60 % sequence identity) needle protein (Demers et al. 2013) is PrgI which also forms T3SS needles. Due to this similarity, its dynamics will be used here to make deductions for the dynamics of MxiH needles. For such a PrgI needle sample (sparsely ^{13}C, uniformly ^{15}N-labeled) (Loquet et al. 2012) the ^{15}N T_1 times were measured to be on average 106 s at 800 MHz ^{1}H Larmor frequency (see Fig. 2 for T_1 times per residue, supplementary material for experimental details). This value is in contrast to other protein systems: For microcrystalline SH3 (uniformly ^{2}H, ^{13}C, ^{15}N-labeled, 10 % back-protonated sample), the corresponding value is 26 s (900 MHz) (Chevelkov et al. 2007; Pauli et al. 2001). For microcrystalline ubiquitin (uniformly ^{2}H, ^{13}C, ^{15}N-labeled, 30 % back-protonated sample), the reported value is 35 s at 850 MHz (average over all residues) (Fasshuber et al. 2015; Schanda et al. 2010). As can be seen, the T_1 relaxation times of the T3SS needles are about four times longer and therefore prove the remarkably low flexibility of the system. This results in a much smaller contribution of inhomogeneous line-broadening under DNP conditions and can serve as an explanation on why the T3SS sample yields good resolution at room temperature and at cryogenic temperatures alike.

It has been shown that ssNMR is a useful tool for the investigation of protein dynamics (Ivanir-Dabora et al. 2015; Lamley et al. 2015; Lewandowski et al. 2015; Ma et al. 2015). In our previous study (Fricke et al. 2014), we found that the peaks of the residues located on the outer surface of the needle are more difficult to identify than those that face towards the needle lumen. This had been attributed to a lower flexibility of the inner residues due to the constraining effect of the needle structure. In contrast, the outer part of the needle has more freedom to move resulting in different conformations that interconvert at room temperature (and thus lead to a single chemical shift). They freeze out at low temperature leading to such severe line-broadening that those residues become unobservable. Another possible explanation of this observation could be that the biradical molecules do not enter the needle so that only the outer residues experience quenching by the proximity of the biradicals (Koers et al. 2014; van der Cruijsen et al. 2015).

To rule out the latter option and to lend further support to our hypothesis that this effect indeed stems from the differing degrees of dynamics at room temperature, ambient temperature ^{13}C-^{13}C PDSD 2D NMR spectra of the pure protein and of the DNP sample (containing the DNP matrix and the biradical) have been compared (Fig. 3). It can be seen that for all peaks the line-widths at half height are generally slightly higher in the spectrum of the AMUPol-containing sample. Nevertheless, it does not

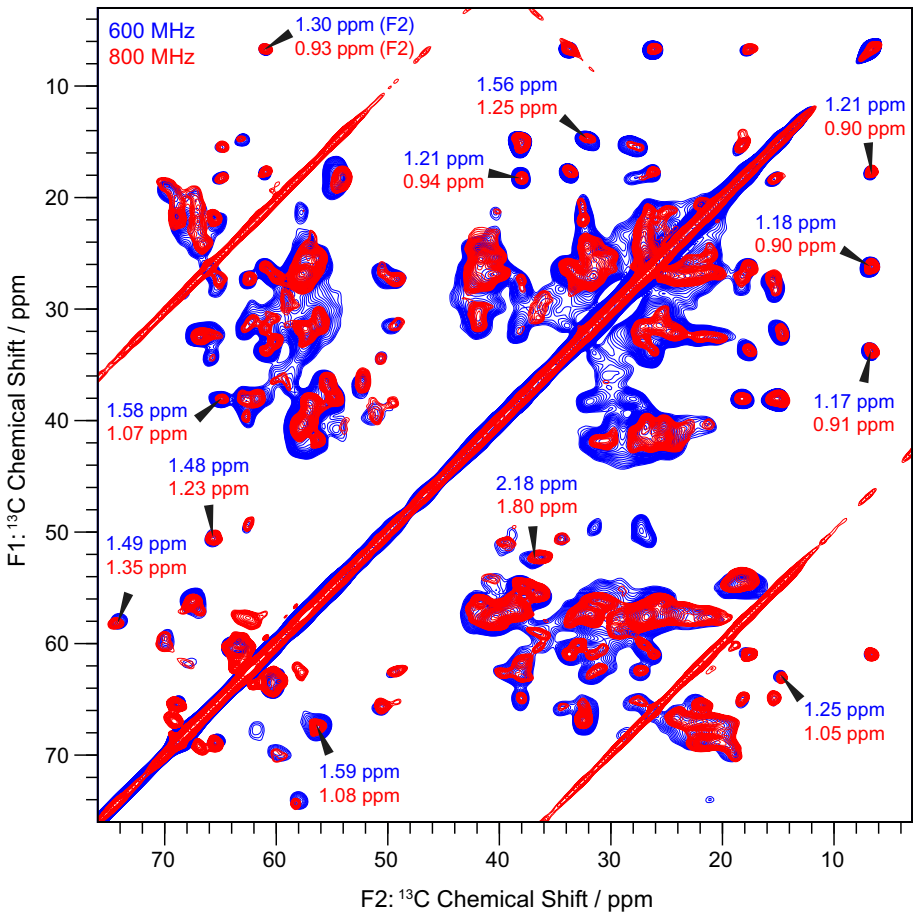

Fig. 1 Overlay of ^{13}C-^{13}C PDSD 2D NMR spectra of MxiH needles using DNP at 800 MHz (*red*, 8 kHz MAS, 95 K, 30 ms mixing time) and at 600 MHz (*blue*, 11 kHz MAS, 104 K, 20 ms mixing time). 45° phase-shifted *squared sine bells* were used as window functions for both spectra. Full line-widths at half height in the direct dimension (F2) are annotated for some resolved peaks illustrating the increase in resolution at 800 MHz. The peaks between 26 and 32 ppm (F2) and 50 ppm (F1) are present in the 800 MHz spectrum (see mirror peaks across diagonal), but are not visible here as they have lower intensity at this side of the diagonal

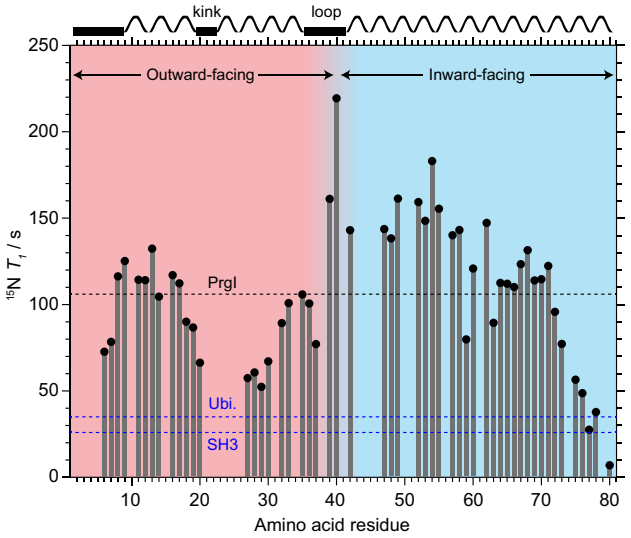

Fig. 2 ^{15}N T_1 times in the homologous T3SS needle with PrgI subunits. The corresponding secondary structure elements are illustrated on top. The averages over all residues are indicated for PrgI needles (average over shown *bars*), ubiquitin and SH3 (*bars* not shown) as *dashed lines*. Note that the residues facing inward (towards the needle lumen) have higher T_1 times (are less flexible) than the ones facing outward

become apparent that the peaks of the outer amino acids (residues 1-39, the N-terminal helix) suffer from more severe line-broadening than the inner amino acids (residues 45-83, the C-terminal helix), as the comparison of the selected 1D-slices illustrates.

There are some peaks that have severely reduced intensity in the AMUPol sample (some annotated in green). These cases are located in the inner and outer parts of the assembly and do not follow any identifiable preference for residue location. The concerned amino acid types are hydrophobic so that it can be assumed that there is a certain interaction with the also slightly hydrophobic biradical. Shifted peaks could be found only for the βγ-correlations of V3 (green box). This residue may possibly form a direct interaction with AMUPol. A more flexible outer part of the needle is further corroborated by the shorter ^{15}N T_1 times of the outward-facing residues in comparison with the inward-facing-residues in the homologous protein PrgI (Fig. 2).

In summary, we found that the already excellent spectral resolution of our macromolecular protein assembly increases significantly going from DNP at 600 MHz to DNP at

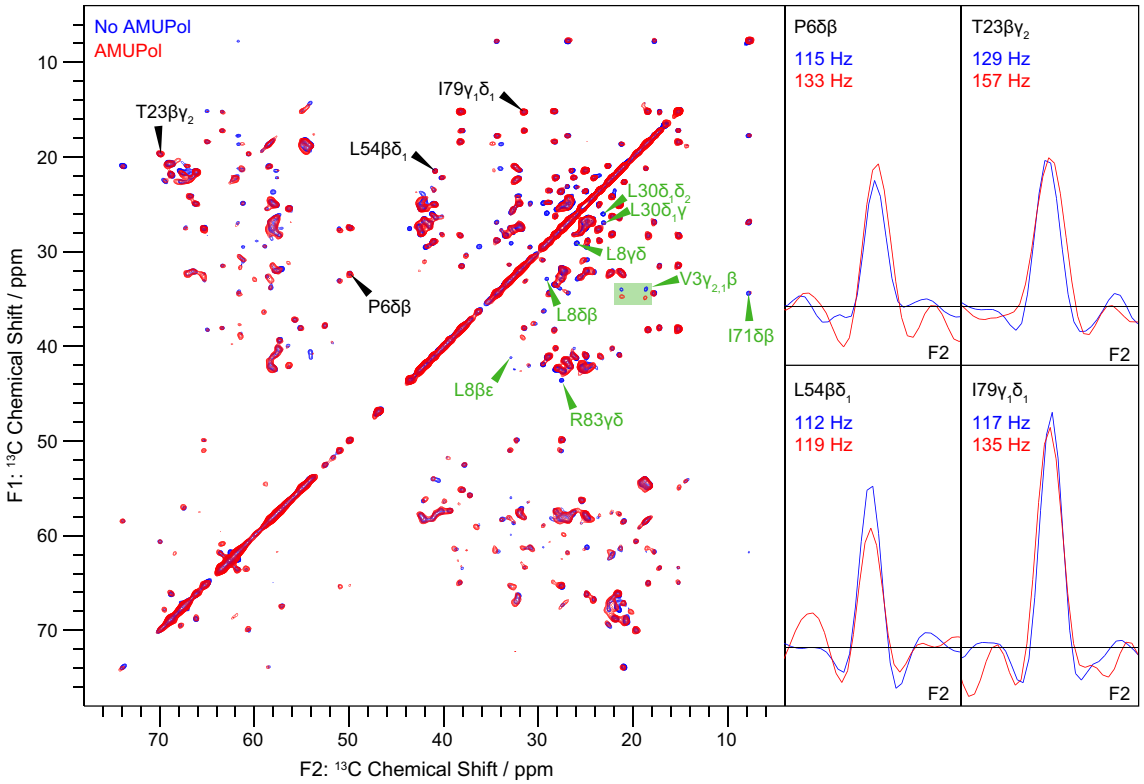

Fig. 3 Overlay of ^{13}C-^{13}C PDSD 2D NMR spectra of MxiH needles at ambient temperature at 800 MHz and 11 kHz MAS. The *blue spectrum* represents the pure protein sample without any biradical (total measurement time: 13 h 30 min); the *red spectrum* is from the sample used for the DNP measurements (same total measurement time) and contains the biradical AMUPol (same sample as the one used to record the *red spectrum* in Fig. 1). 1D traces through the annotated peaks (*black*) are shown on the right. They compare the different peak widths at half height (FWHH) for the two NMR spectra. The *green* annotations represent peaks which have severely diminished intensity in the AMUPol spectrum in comparison with the biradical-free spectrum. The two valine peaks in the *green box* are shifted in terms of the Cβ chemical shift

800 MHz. This is attributed to the overall very low flexibility of the structure which leaves homogeneous line-broadening as the main cause for the broad peaks at cryogenic temperatures—an effect that decreases with increasing field strength. For crowded protein NMR spectra, the resolution is a determining factor, so this increase is a substantial benefit. The lower DNP enhancement factor at higher magnetic fields (Mance et al. 2015) can therefore be a reasonable compromise as the information content in the spectra increases and the sensitivity loss due to line-broadening is reduced—an effect that becomes important when recording 3D spectra required for resonance assignment.

We also found that at ambient temperature the line-broadening due to the presence of the biradical is not significantly different for inner and outer helix residues. This supports the notion that the spectral differences between inner and outer parts of the needle observed using DNP at low temperature are not the result of the absence of biradical inside the needles, but rather represent true differences in conformational plasticity at room temperature.

Acknowledgments We thank Brigitta Angerstein for technical help, and Maximilian Zinke and Eve Ousby for valuable discussions. This work was supported by the Leibniz-Institut für Molekulare Pharmakologie, the Max Planck Society, the European Research Council (ERC Starting Grant to A.L.), the German Research Foundation (Deutsche Forschungsgemeinschaft; Emmy Noether Fellowship to A.L.) and the Fonds der Chemischen Industrie (Kekulé Scholarship to P.F.). Work at the 800 MHz DNP instrument at Utrecht was supported by NWO (Grants 700.11.344 and 700.58.102 to M.B.).

References

Barnes AB, Paepe GD, van der Wel PC, Hu KN, Joo CG, Bajaj VS, Mak-Jurkauskas ML, Sirigiri JR, Herzfeld J, Temkin RJ, Griffin RG (2008) High-field dynamic nuclear polarization for solid and solution biological NMR. Appl Magn Reson 34:237–263. doi:10.1007/s00723-008-0129-1

Becker-Baldus J, Bamann C, Saxena K, Gustmann H, Brown LJ, Brown RC, Reiter C, Bamberg E, Wachtveitl J, Schwalbe H, Glaubitz C (2015) Enlightening the photoactive site of channelrhodopsin-2 by DNP-enhanced solid-state NMR spectroscopy. Proc Natl Acad Sci USA 112:9896–9901. doi:10.1073/pnas.1507713112

Can TV, Ni QZ, Griffin RG (2015) Mechanisms of dynamic nuclear polarization in insulating solids. J Magn Reson 253:23–35. doi:10.1016/j.jmr.2015.02.005

Chevelkov V, Zhuravleva AV, Xue Y, Reif B, Skrynnikov NR (2007) Combined analysis of (15)N relaxation data from solid- and solution-state NMR spectroscopy. J Am Chem Soc 129:12594–12595. doi:10.1021/ja073234s

Debelouchina GT, Bayro MJ, Fitzpatrick AW, Ladizhansky V, Colvin MT, Caporini MA, Jaroniec CP, Bajaj VS, Rosay M, Macphee CE, Vendruscolo M, Maas WE, Dobson CM, Griffin RG (2013) Higher order amyloid fibril structure by MAS NMR and DNP spectroscopy. J Am Chem Soc 135:19237–19247. doi:10.1021/ja409050a

Del Amo JML, Schneider D, Loquet A, Lange A, Reif B (2013) Cryogenic solid state NMR studies of fibrils of the Alzheimer's disease amyloid-beta peptide: perspectives for DNP. J Biomol NMR 56:359–363. doi:10.1007/s10858-013-9755-5

Demers JP, Sgourakis NG, Gupta R, Loquet A, Giller K, Riedel D, Laube B, Kolbe M, Baker D, Becker S, Lange A (2013) The common structural architecture of Shigella flexneri and Salmonella typhimurium type three secretion needles. PLoS Pathog 9:e1003245. doi:10.1371/journal.ppat.1003245

Demers JP, Habenstein B, Loquet A, Vasa SK, Giller K, Becker S, Baker D, Lange A, Sgourakis NG (2014) High-resolution structure of the *Shigella* type-III secretion needle by solid-state NMR and cryo-electron microscopy. Nat Commun 5:4976. doi:10.1038/ncomms5976

Fasshuber HK, Lakomek NA, Habenstein B, Loquet A, Shi C, Giller K, Wolff S, Becker S, Lange A (2015) Structural heterogeneity in microcrystalline ubiquitin studied by solid-state NMR. Protein Sci 24:592–598. doi:10.1002/pro.2654

Fricke P, Demers JP, Becker S, Lange A (2014) Studies on the MxiH protein in T3SS needles using DNP-enhanced ssNMR spectroscopy. Chem Phys Chem 15:57–60. doi:10.1002/cphc.201300994

Fricke P, Chevelkov V, Shi C, Lange A (2015) Strategies for solid-state NMR investigations of supramolecular assemblies with large subunit sizes. J Magn Reson 253:2–9. doi:10.1016/j.jmr.2014.10.018

Gupta R, Lu M, Hou G, Caporini MA, Rosay M, Maas W, Struppe J, Suiter C, Ahn J, Byeon IJ, Franks WT, Orwick-Rydmark M, Bertarello A, Oschkinat H, Lesage A, Pintacuda G, Gronenborn AM, Polenova T (2016) Dynamic nuclear polarization enhanced MAS NMR spectroscopy for structural analysis of HIV-1 protein assemblies. J Phys Chem B 120:329–339. doi:10.1021/acs.jpcb.5b12134

Hohwy M, Rienstra CM, Jaroniec CP, Griffin RG (1999) Fivefold symmetric homonuclear dipolar recoupling in rotating solids: application to double quantum spectroscopy. J Chem Phys 110:7983–7992. doi:10.1063/1.478702

Ivanir-Dabora H, Nimerovsky E, Madhu PK, Goldbourt A (2015) Site-resolved backbone and side-chain intermediate dynamics in a carbohydrate-binding module protein studied by magic-angle spinning NMR spectroscopy. Chemistry 21:10778–10785. doi:10.1002/chem.201500856

Kaplan M, Cukkemane A, van Zundert GC, Narasimhan S, Daniels M, Mance D, Waksman G, Bonvin AM, Fronzes R, Folkers GE, Baldus M (2015) Probing a cell-embedded megadalton protein complex by DNP-supported solid-state NMR. Nat Methods 12:649–652. doi:10.1038/nmeth.3406

Koers EJ, van der Cruijsen EA, Rosay M, Weingarth M, Prokofyev A, Sauvee C, Ouari O, van der Zwan J, Pongs O, Tordo P, Maas WE, Baldus M (2014) NMR-based structural biology enhanced by dynamic nuclear polarization at high magnetic field. J Biomol NMR 60:157–168. doi:10.1007/s10858-014-9865-8

Lamley JM, Oster C, Stevens RA, Lewandowski JR (2015) Intermolecular interactions and protein dynamics by solid-state NMR spectroscopy. Angew Chem Int Ed 54:15374–15378. doi:10.1002/anie.201509168

Lee D, Hediger S, De Paepe G (2015) Is solid-state NMR enhanced by dynamic nuclear polarization? Solid State Nucl Magn Reson 66–67:6–20. doi:10.1016/j.ssnmr.2015.01.003

Lelli M, Chaudhari SR, Gajan D, Casano G, Rossini AJ, Ouari O, Tordo P, Lesage A, Emsley L (2015) Solid-state dynamic nuclear polarization at 9.4 and 18.8 T from 100 K to room temperature. J Am Chem Soc 137:14558–14561. doi:10.1021/jacs.5b08423

Lewandowski JR, Halse ME, Blackledge M, Emsley L (2015) Protein dynamics. Direct observation of hierarchical protein dynamics. Science 348:578–581. doi:10.1126/science.aaa6111

Liao SY, Lee M, Wang T, Sergeyev IV, Hong M (2016) Efficient DNP NMR of membrane proteins: sample preparation protocols, sensitivity, and radical location. J Biomol NMR. doi:10.1007/s10858-016-0023-3

Linden AH, Franks WT, Akbey U, Lange S, van Rossum BJ, Oschkinat H (2011) Cryogenic temperature effects and resolution upon slow cooling of protein preparations in solid state NMR. J Biomol NMR 51:283–292. doi:10.1007/s10858-011-9535-z

Loquet A, Sgourakis NG, Gupta R, Giller K, Riedel D, Goosmann C, Griesinger C, Kolbe M, Baker D, Becker S, Lange A (2012) Atomic model of the type III secretion system needle. Nature 486:276–279. doi:10.1038/nature11079

Ma P, Xue Y, Coquelle N, Haller JD, Yuwen T, Ayala I, Mikhailovskii O, Willbold D, Colletier JP, Skrynnikov NR, Schanda P (2015) Observing the overall rocking motion of a protein in a crystal. Nat Commun 6:8361. doi:10.1038/ncomms9361

Mance D, Gast P, Huber M, Baldus M, Ivanov KL (2015) The magnetic field dependence of cross-effect dynamic nuclear polarization under magic angle spinning. J Chem Phys 142:234201. doi:10.1063/1.4922219

Ni QZ, Daviso E, Can TV, Markhasin E, Jawla SK, Swager TM, Temkin RJ, Herzfeld J, Griffin RG (2013) High frequency dynamic nuclear polarization. Acc Chem Res 46:1933–1941. doi:10.1021/ar300348n

Pauli J, Baldus M, van Rossum B, de Groot H, Oschkinat H (2001) Backbone and side-chain 13C and 15 N signal assignments of the alpha-spectrin SH3 domain by magic angle spinning solid-state NMR at 17.6 Tesla. ChemBioChem 2:272–281

Perras FA, Reinig RR, Slowing II, Sadow AD, Pruski M (2016) Effects of biradical deuteration on the performance of DNP: towards better performing polarizing agents. Phys Chem Chem Phys 18:65–69. doi:10.1039/c5cp06505d

Potapov A, Yau WM, Ghirlando R, Thurber KR, Tycko R (2015) Successive stages of Amyloid-beta self-assembly characterized by solid-state nuclear magnetic resonance with dynamic nuclear polarization. J Am Chem Soc 137:8294–8307. doi:10.1021/jacs.5b04843

Rosay M, Tometich L, Pawsey S, Bader R, Schauwecker R, Blank M, Borchard PM, Cauffman SR, Felch KL, Weber RT, Temkin RJ, Griffin RG, Maas WE (2010) Solid-state dynamic nuclear polarization at 263 GHz: spectrometer design and experimental results. Phys Chem Chem Phys 12:5850–5860. doi:10.1039/c003685b

Sauvee C, Rosay M, Casano G, Aussenac F, Weber RT, Ouari O, Tordo P (2013) Highly efficient, water-soluble polarizing agents for dynamic nuclear polarization at high frequency. Angew Chem Int Ed 52:10858–10861. doi:10.1002/anie.201304657

Schanda P, Meier BH, Ernst M (2010) Quantitative analysis of protein backbone dynamics in microcrystalline ubiquitin by solid-state

NMR spectroscopy. J Am Chem Soc 132:15957–15967. doi:10.1021/ja100726a

Shi C, Fricke P, Lin L, Chevelkov V, Wegstroth M, Giller K, Becker S, Thanbichler M, Lange A (2015) Atomic-resolution structure of cytoskeletal bactofilin by solid-state NMR. Sci Adv 1:e1501087. doi:10.1126/sciadv.1501087

Siemer AB, Huang KY, McDermott AE (2012) Protein linewidth and solvent dynamics in frozen solution NMR. PLoS One 7:e47242. doi:10.1371/journal.pone.0047242

Song C, Hu KN, Joo CG, Swager TM, Griffin RG (2006) TOTAPOL: a biradical polarizing agent for dynamic nuclear polarization experiments in aqueous media. J Am Chem Soc 128:11385–11390. doi:10.1021/ja061284b

Su Y, Andreas L, Griffin RG (2015) Magic angle spinning NMR of proteins: high-frequency dynamic nuclear polarization and (1)H detection. Annu Rev Biochem 84:465–497. doi:10.1146/annurev-biochem-060614-034206

Takahashi H, Lee D, Dubois L, Bardet M, Hediger S, De Paepe G (2012) Rapid natural-abundance 2D 13C-13C correlation spectroscopy using dynamic nuclear polarization enhanced solid-state NMR and matrix-free sample preparation. Angew Chem Int Ed 51:11766–11769. doi:10.1002/anie.201206102

Takahashi H, Hediger S, De Paepe G (2013) Matrix-free dynamic nuclear polarization enables solid-state NMR 13C-13C correlation spectroscopy of proteins at natural isotopic abundance. Chem Commun 49:9479–9481. doi:10.1039/c3cc45195j

van der Cruijsen EA, Koers EJ, Sauvee C, Hulse RE, Weingarth M, Ouari O, Perozo E, Tordo P, Baldus M (2015) Biomolecular DNP-supported NMR spectroscopy using site-directed spin labeling. Chemistry 21:12971–12977. doi:10.1002/chem.201501376

Zagdoun A, Casano G, Ouari O, Schwarzwalder M, Rossini AJ, Aussenac F, Yulikov M, Jeschke G, Coperet C, Lesage A, Tordo P, Emsley L (2013) Large molecular weight nitroxide biradicals providing efficient dynamic nuclear polarization at temperatures up to 200 K. J Am Chem Soc 135:12790–12797. doi:10.1021/ja405813t